Hotspot Condition Analysis and Proposed Hotspot Detection Method for the PV Module in Cluster's Structure

Jirada Gosumbonggot[1]*

[1*]*Department of Electrical Engineering, Faculty of Engineering, Thai-Nichi Institute of Technology, Bangkok, Thailand*

*Corresponding Author. E-mail address: jirada@tni.ac.th

Received: 30 April 2021; Revised: 29 May 2021; Accepted: 10 June 2021
Published online: 25 June 2021

Abstract

Renewable energy becomes an emerging trend in many countries. Photovoltaic (PV) technology has been gaining an increasing amount of attention due to its unpolluted operation. Importantly, the PV system should be utilized with safety awareness. The problem of hotspot takes place due to the mismatch in the irradiation of the cells in the PV module. Under the hotspot condition, the unshaded part of the module operates at a current level higher than the shaded cell. As a result, the affected cells start to dissipate power leading to an increase in the temperature. Afterward, the hotspot reduces performance and brings damage to the PV module. This paper presents the hotspot detection algorithm that can integrate with the PV's MPPT system. The method uses the concept of characteristic curves analysis and the rate of current changes under reversed bias conditions to detect the hotspot. Moreover, the algorithm displays the PV system's status indicator after the detection completes. The implementations in different testing cases, including various PV sizing at different irradiation levels. Results confirm the performance of the proposed algorithm, showing the accuracy with fast detection.

Keywords: Photovoltaic, Hotspot detection, Shading condition, Irradiation

I. INTRODUCTION

Renewable power led by photovoltaic (PV) technology has gained popularity as one of the potential avenues. PV's expansion increases due to unlimited power resources from the sunlight and unpolluted operation with no emission. Researches in renewable energy receive great attention. Because most of the resources are available on short-timescales and depend on the weather conditions, it is important to investigate the enhancement of renewable energy to achieve its highest potential. To enhance the efficiency of PV, the effect of weather conditions must be considered. Two main parameters affect the PV-generated power, irradiation and temperature; they vary from the location where the PV is installed. Moreover, the problems that could occur to the PV system such as cell mismatch, material degradation and shading could lead to a problem called a hotspot.

A hotspot is defined as the fault formed on the panel's surface, which happens from the consequence of shading on the PV panel's surface when a PV cell in a panel generates less power. Hotspot not only causes the generated power reduction but could also lead to a PV cell's damage. Conventionally, the detection uses the infrared camera to capture a thermal image of objects under inspection [1]. Although the thermography detection method's performance is effective, the cost of the equipment especially the infrared camera is generally quite high, and a workforce for the routine checkup is also needed. Although the hotspot happens on a part of the area on the PV cell, the power dissipation caused by the temperature can be found.

In addition, it is confirmed by case studies and surveys that hotspot causes the reduction of PV system's performance ratio. Work done by Dhimish et al. [2] presents the impact of hotspot through the PV modules installed across the U.K. The study shows that 42% of all the installed PV modules do contain the hotspot. The existed hotspot causes a -15.47% decrease rate of the performance ratio, making the generated power of the PV system decreases every year. Other confirmations are shown by Pillai et al., Hossam et al. and Yedidi et al. [3]–[5] show that hotspots can cause a reduction of energy yields up to 15%. According to the studies, researchers need to develop methods for detecting hotspots accurately and effectively.

The main context of this paper is to describe the effect of the hotspot by the operation factors and propose the hotspot detection methodology for the small-scale PV system, in the form of the algorithm. The analysis of hotspots in each condition is performed and verified with the description explained by the IEC 61215 standard. The hotspot detection method is designed based on the practical PV module model with the three clusters structure. The proposed algorithm operates using the real-time difference method (RDM) [6] by sensing real-time voltage and current from the PV module. After that, the real-time calculation of PV output parameters and comparison with the reference values are performed. The algorithm is designed by using the analysis from the PV's characteristic curve and the rate of current changes under reversed bias conditions to detect the hotspot. After the detection completes, the algorithm displays the PV module's status by using the indicator signal. The usefulness of this research is the presented algorithm can accurately detect the hotspot and differentiate it from normal and shading conditions. The proposed method shows the compatibility with the practical PV standard.

II. PROBLEM STATEMENT

The hotspot is formed by the localized heat on the PV module's surface, which happens due to the mismatch in the PV cell, shading or material defection [7]–[8]. During the hotspot condition, the PV cell

voltage operates in reversed bias. Instead of generating the power, the hotspot cell starts to absorb the current generated from other normal condition cells. Then, the total power generated from the PV module is reduced and the temperature inside the cell increases. If the temperature reaches and exceeds the limited threshold (85 ºC typical rate for PV to operate and at 150 ºC for the permanent damage), [1] the hotspot can be formed and bring permanent damage to the module.

The efficiency degradation of the PV module due to the hotspot has been confirmed by research works [9]–[11]. In practice, the PV module internal structure contains the PV cells arranged in series connection, the cells are divided into a group called a cluster. In each cluster, the bypass diode is installed to prevent the extreme reverse voltage bias on the PV module. Figure 1 shows the PV module in three cluster structures with one hotspot's cell highlighted.

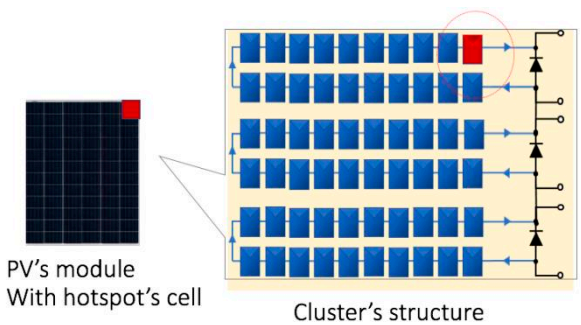

Figure 1 Hotspot's cell in PV module model in three cluster's structure [12]

To decrease the effect of shading towards the hotspot, bypass diodes are installed. Diodes can restrain the reverse bias voltage that can occur in a PV cell, and protect the cell's current to reach the breakdown voltage by providing the alternative path for the current to flow. However, studies show the disadvantages in the case of the long-term operation, higher temperature, and the installation generates maximum power points alignment which increases the difficulty to track PV's highest power [2], [12]–[14].

Detailed confirmation is explained in IEC 61215 (design qualification and type approval of PV module) [15]. The standard states the hotspot endurance testing method to determine the ability of the module to withstand hotspot heating effects. When the hotspot's cell exists in the module, the cell's current inclines significantly and the total module current starts to decrease. The fundamental simulation in Figure 2 is performed to present the effect of the hotspot, according to the information in IEC 61215.

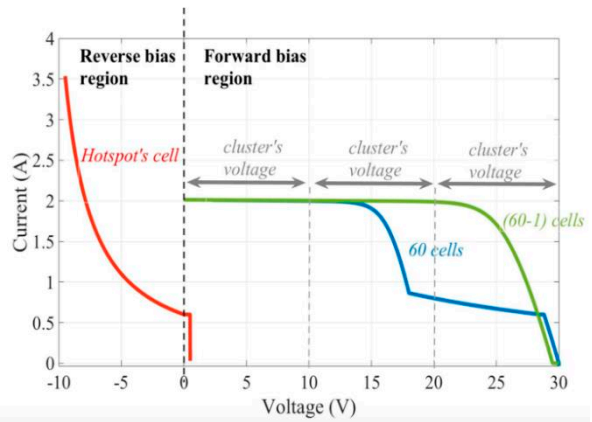

Figure 2 I-V characteristic curves of the hotspot's cell and whole PV module [15]

By using the configuration in Figure 1, the current-voltage characteristic of the hotspot's cell and total PV module under normal and hotspot conditions are displayed. The simulation uses the testing condition according to the IEC 61215 standard. The hotspot's cell is set to have the irradiation of 300 W/m^2, while other cells operate at 1000 W/m^2. The results present three current parameters measured at the hotspot's cell, the normal condition cells and the whole PV module. The voltage is divided into two regions include the forward bias (PV's voltage is greater than zero) and the reverse bias (PV's voltage is less than zero). Under reversed bias region, the red graph displays the hotspot cell's current

which increased exponentially, starts from 0.5 A which indicates the PV's current value at 300 W/m^2. The current continues to increase until it reaches the breakdown voltage at -10 V.

For the performance of the whole PV module, the blue graph displays the whole PV module's current; which decreases due to the low irradiance on the hotspot's cell. The current drops from the short-circuit current at 2 A to 0.5 A, the drop exists at approximately the PV cluster's voltage (20 V). The result shows that, although the maximum power of the module is not significantly different compared to the normal condition, the power dissipation is hidden under the hotspot's cell which causes the cell to overheat and bring damage. The IEC 61215 standard clearly states the step-by-step testing procedure in which manufactured PV module needs to pass before being certified. IEC 61215 specifically states the hotspot test requirements of the module; however, the hotspot detection procedures have not been described yet. As a result, it is important to study the impact of the hotspot and design the detection method for preventing the damage that occurs to the PV module.

III. ANALYSIS

There are examples of hotspot models presented in published works, represents using DC or AC circuits. In this paper, the model by [16] is used due to its representation in DC which is well-matched to the previously proposed maximum power point tracking (MPPT) algorithm. The model is implemented based on the single-diode DC model with the additional voltage-controlled current source (VCCS) connected to the shunt resistance branch. The reversed bias current I_{BR} is generated, as shown in Figure 3.

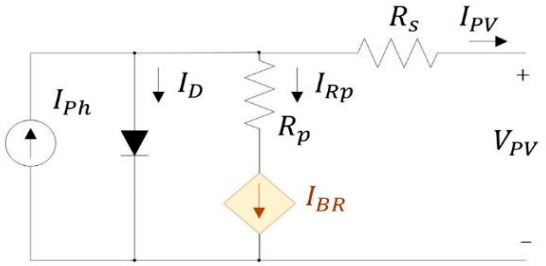

Figure 3 Hotspot model with VCCS and shunt resistance [16]

Equation (1) shows the expression of the currents in the circuit according to Kirchoff's current law.

$$I_{PV} = I_{ph} - I_D - I_{Rp} \quad (1)$$

The current I_{BR} generated from the additional VCCS is expressed as shown in equation (2) [16]. From equation (2), α and m are the fitting parameter (α=1.93 and m=1.10 for the crystalline Silicon) and V_{BD} is the cell's breakdown voltage.

$$I_{BR} = \begin{cases} 0 & , V_{PV} > 0 \\ \alpha\left(\frac{V_{PV}}{R_p}\right)\left(1 - \left(\frac{V_{PV}}{V_{BD}}\right)\right)^{-m} & , V_{PV} \leq 0 \end{cases} \quad (2)$$

When V_{PV} turns negative, the current source generates I_{BR} in the exponential trends. As described in section II, since the material's degradation in the cell can affect the hotspot model parameter and increase the induced current; therefore, the analysis considers the effect of the shunt resistance towards the performance of the PV module. A detailed investigation is performed by considering the value of shunt resistance (R_P), and levels of irradiation as shown in at different irradiations Figure 4.

.

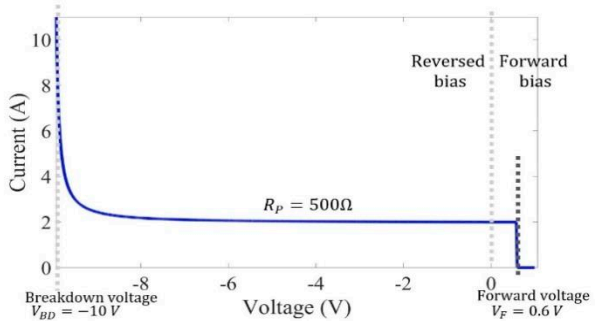

(a) At certain shunt resistance

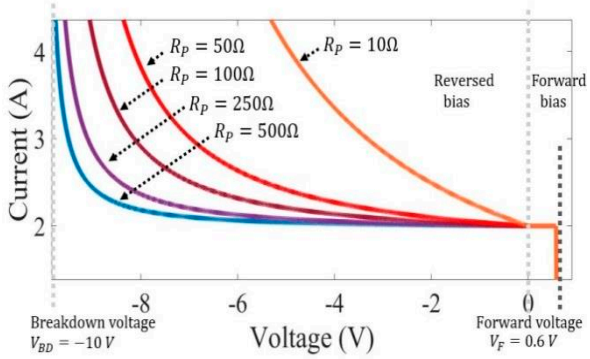

(b) At different shunt resistances

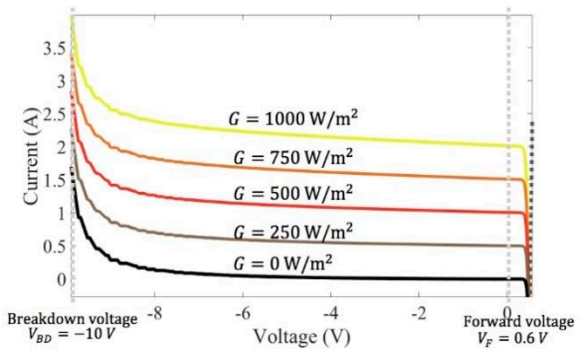

(c) At different irradiations

Figure 4 I-V characteristic curves of the hotspot cell

As shown in figure 4a, under the forward bias condition the cell's diode turns on when reaching the diode's forward voltage V_F of 0.6 V. PV's current I_{PV} increases to approximately 2 A. In contrast to the reverse bias condition, the graph shows the PV's current starts to incline exponentially, especially when reaching the breakdown voltage of 10 V. Overall, in figure 4b the result presents the generation of a large current from the low resistances. Especially for the lowest resistance value of 10 Ohm, the current increases significantly at approximately -5 V, which the voltage is less than the value of the breakdown voltage. The low resistance value can be reflected as the degradation which induces more current and more power dissipation. Also, due to the dependence of weather, especially irradiation, it is necessary to evaluate the hotspot effect at different irradiation levels. Figure 4c shows that the more irradiation inputs to the hotspot's cell, the more generated current causes a higher power dissipation.

IV. METHODOLOGY

The system in Figure 5 is implemented by PV array (two series-connected modules, one module contains the hotspot's cell), the boost converter with a duty cycle control and the constant voltage load.

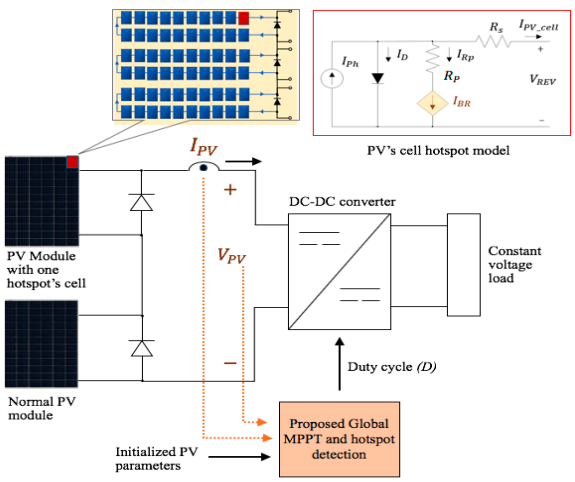

Figure 5 System's implementation

The results achieved from the system's implementation in figure 6 are used to design the algorithm.

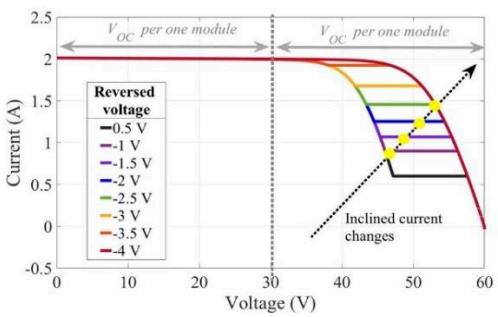

(a) I-V characteristic curves under hotspot condition

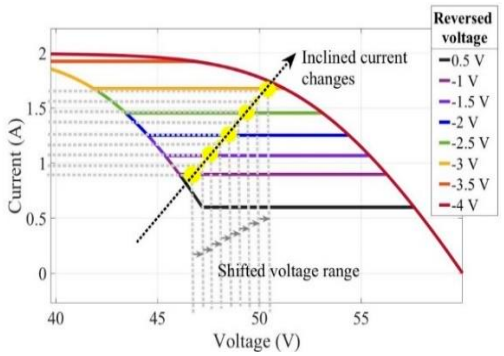

(b) Magnified inclined current changes detection area

Figure 6 I-V characteristic curves under hotspot condition with the decrease of reverse bias voltage over time

From figure 6, levels of reversed voltages are set to be between -0.5 V to -4 V with the decrement of 0.5 V, to present the behavior of the hotspot while the reversed voltages approaching the breakdown voltage. The characteristic curves undervalue of reversed voltage are displayed. The condition shows the amount of PV's current at different reversed voltage. The less reversed voltage, the more increased the current is displayed.

The proposed hotspot detection method is shown in (b) Figure 7. The algorithm is designed by using the slope calculation concept to identify the hotspot. The program has two major parts (a) the main program and (b) the hotspot detection algorithm. The main improvement is the compatibility with the practical cluster structure. Furthermore, to increase the functionality, the algorithm is also complemented with the shading detection and global MPP tracking system. The tracking algorithm has published by the author [17].

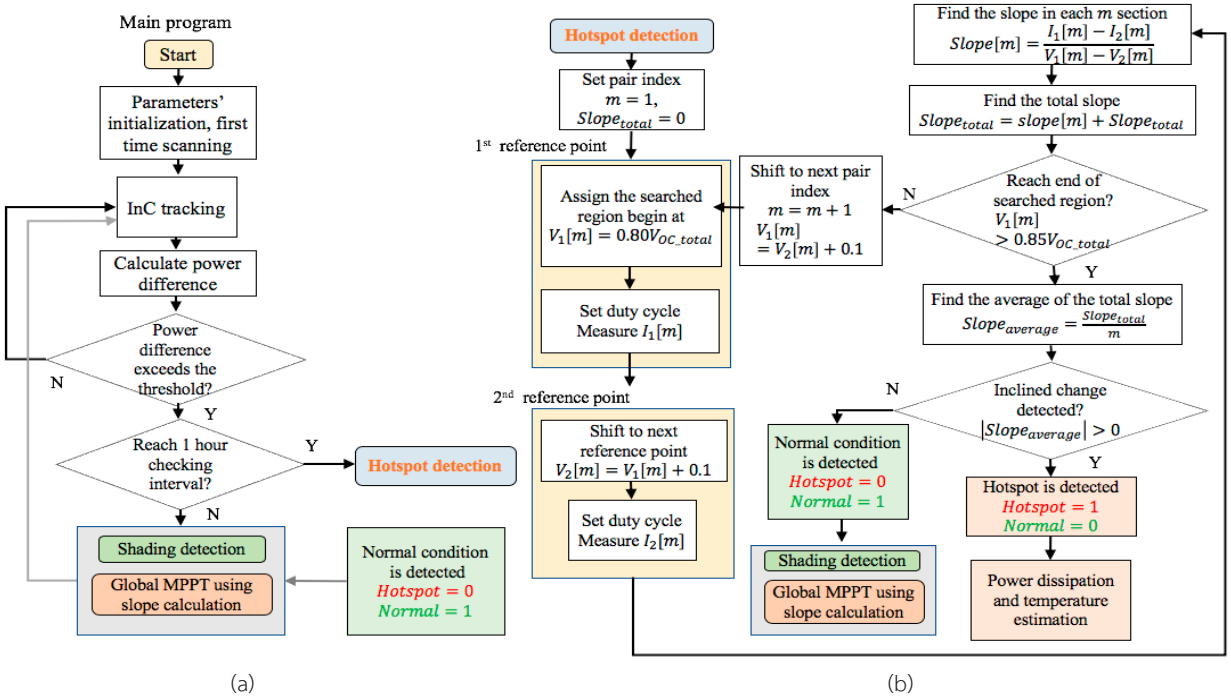

(a) (b)

Figure 7 Proposed hotspot detection algorithm for PV module in cluster's structure
(a) The main program (b) Hotspot detection

From the I-V characteristic curves, the commonly searched region for all number of defected clusters locates at the ranges of the knee level of the curve (at 80% of PV's open-circuit voltage (V_{OC})). Consequently, the algorithm starts detecting the inclined current from 80% of V_{OC}. The measured

voltage is assigned as the first reference voltage $V_1[1]$ and the current is recorded as $I_1[1]$. Step repeats after shifting the voltage by 0.1 V to the next point $V_2[1]$ at 85% of V_{OC}; afterward, the algorithm records the current $I_2[1]$. Consequently, the algorithm calculates the rate of change called $Slope[m]$ between two current points with respect to the voltage points. The calculation is shown in equation (3).

$$Slope[m] = \frac{(I_2[m]-I_1[m])}{(V_2[m]-V_1[m])} \quad (3)$$

After calculating the slope pairs in the searched region, the average of the total slope ($|Slope_{average}|$) is determined. The algorithm calculates whether $|Slope_{average}|$ presents the increase of PV's current inside the hotspot's cell. If $|Slope_{average}|$ shows the inclined trend (value is greater than 0), the program estimates the status as the hotspot condition, making the hotspot indicator triggers from 0 to 1. After that, the algorithm proceeds to the second stage which is the power dissipation and temperature estimation. On the other hand, if $|Slope_{average}|$ does not show the increase of PV's current (value is less than or equal to zero), meaning the PV cell does not present the hotspot characteristic.

The proposed algorithm uses the indicator to present the detection result. Two indicators are “Hotspot” and “Normal”. The hotspot indicator shows when the hotspot is detected. Inversely, the normal indicator presents the normal operation. Continuously, the system proceeds to the global MPPT function to track the power back to the highest point. In conclusion, the proposed detection method using slope calculation helps the system to detect the hotspot that occurs in the PV array, also provides the integration with the proposed algorithm to the MPPT. Moreover, the program can track the global MPP after shading happens. After the estimation, the important point is to identify the degradation level regarding the hotspot’s temperature (explained in section II). If the estimated temperatures surpass 150 ºC, the maintenance step should be performed to prevent the severity of the hotspot formation.

V. RESULTS AND DISCUSSION

The implementation is built for evaluating the proposed detection method. The PV cell with the maximum power at 0.76 W, shunt resistance of 35.54 Ohm and series resistance at 0.02 Ohm are used. The implementation in Figure 5 is simulated to detect the proposed detection algorithm. The hotspot's cell is highlighted in red. For testing the algorithm, case studies criteria are referenced from Dhimish et al. work [2], in which cases are divided with five possible values of shunt resistances with a -20% variation with respect to its nominal value. The variation is used to represent different hotspot degradation values. The resistance values include 7, 14, 21, 28 and 35 Ohm. The conditions represent the degradation at different impurity concentrations [16]. Figure 8 presents the results of hotspot detection with the maximum and minimum shunt resistances, including the shading condition.

The results in Figure 8 confirm the efficiency of the proposed hotspot detection algorithm. The program starts with the first time MPPT to determine the maximum power of the total PV array, detecting at 72.74 W. The process takes approximately 2.5 seconds. Continuously, when the hotspot occurs at 10 seconds, the program starts to identify the hotspot by calculating $Slope[m]$ and detecting any incline of the current from the reverse bias current. The result shows the detected slope results. Less shunt resistance develops a higher slope.

Although the resistances vary the changes of PV cell current; the algorithm is capable to detect the incline change. After detection completes, the status indicator triggers from 0 to 1 for indication. The process takes approximately 2.23 seconds. Figures 8a to 8e show the detected slope results. Less shunt resistance develops a higher slope. Although the resistances vary the changes of PV cell current; the algorithm is capable to detect the incline change. After detection completes, the status indicator triggers from 0 to 1 for indication. The process takes approximately 2.23 seconds.

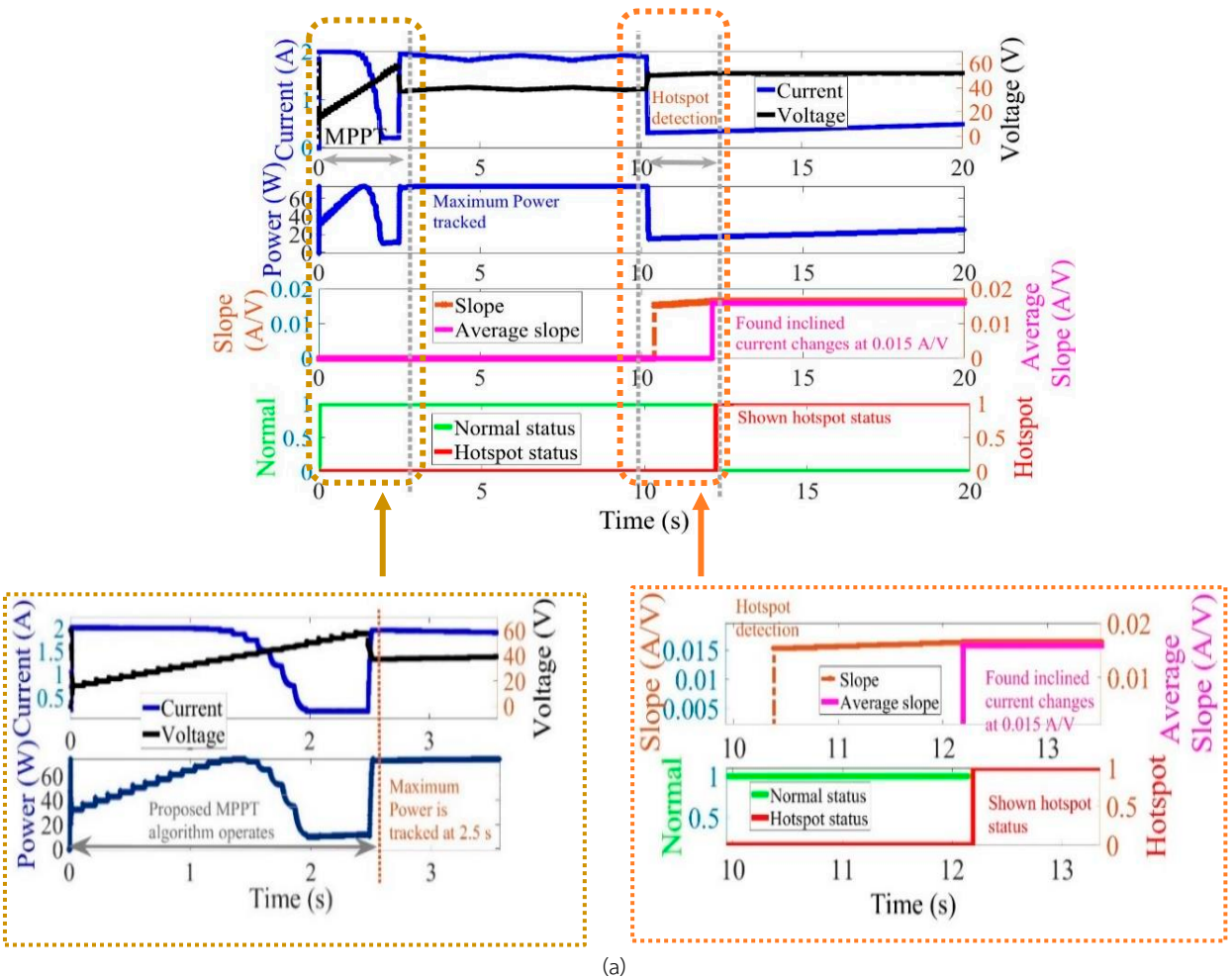

(a)

(b)

(c)

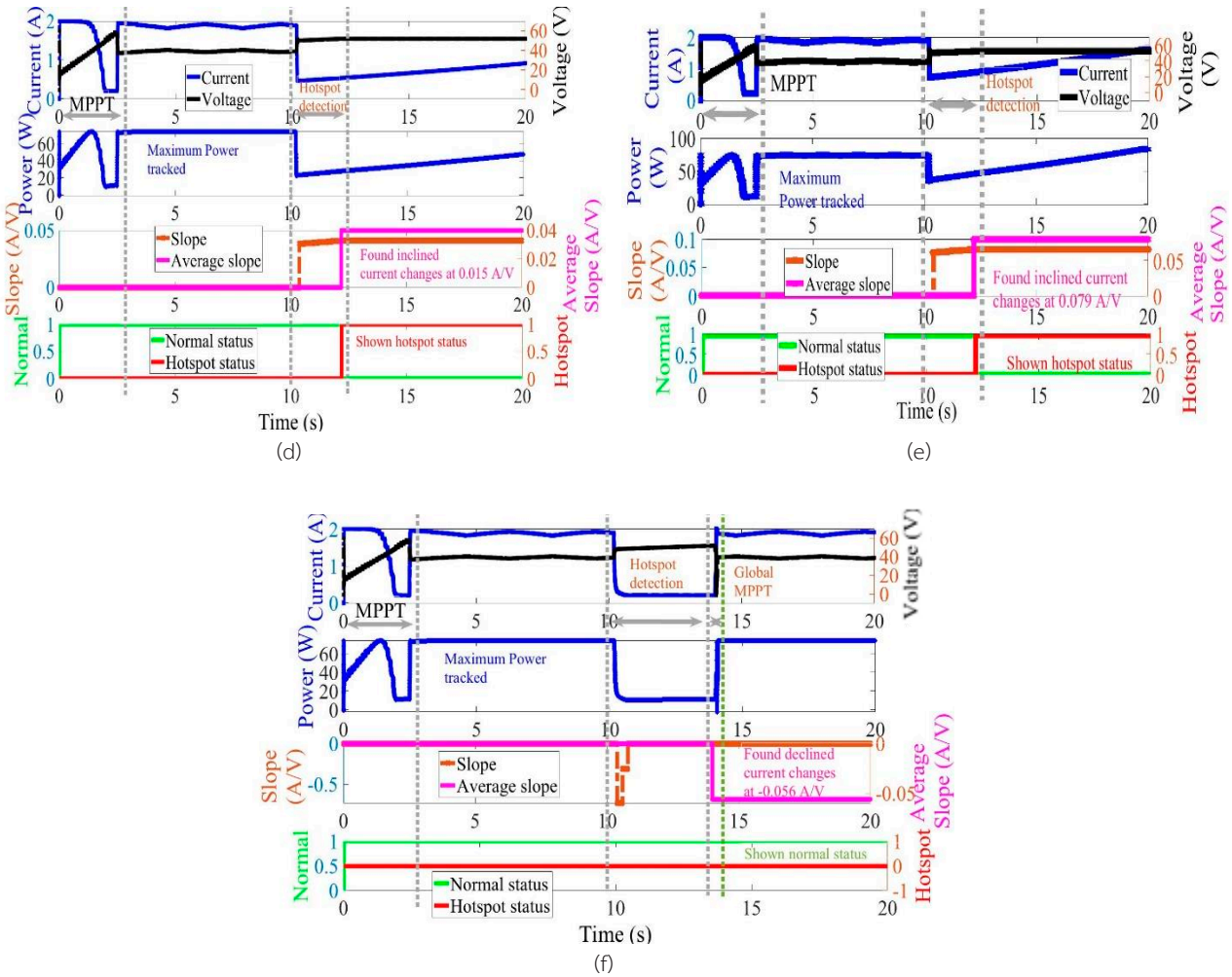

Figure 8 Graphical results of one-cell hotspot detection for shunt resistance cases
(a) 35 Ohm (b) 28 Ohm (c) 21 Ohm (d) 14 Ohm (e) 7 Ohm and (f) shading condition

On the other hand, the proposed algorithm can detect the occurrence of shading conditions. From figure 8f, the results show the detection of the normal condition with the decline slope at -0.15 A/V. The negative slope occurs due to the high parallel resistance in the healthy PV cell. Consequently, the system proceeds to the global MPPT algorithm to restore the power to the maximum level. The algorithm takes approximately 0.23 seconds to track the new global MPP.

Moreover, the proposed method is compared to other published hotspot detection techniques. In this case, the detection based on the real-time difference method is focused. Selected works include the hotspot index determination [12] and equivalent DC resistance and Thevenin impedance calculation [18]. Table I shows the comparison of hotspot detection techniques in terms of implementation requirement and detection capability.

Table 1 Comparison of hotspot detection techniques based on real time difference method

References	Hotspot detection techniques	Implementation requirement	Hotspot detection capability	Remarks
Proposed method	Reversed bias detection from the I-V curve	one current sensor and one voltage sensor	Can detect the hotspot in cell's scale	-
[12]	Hotspot Index determination using PV voltage's ratio	Sensor's number is proportional to number of tested and values of shunt and series resistance	Can detect the hotspot in cell's scale but at certain irradiation	• Test condition is limited to two cluster panels • Hard to distinguish from the shading condition
[18]	Equivalent DC resistance and Thevenin impedance calculation	two current sensors and one voltage sensor	Can detect the hotspot in cell's scale but limited to series-connected configuration	Threshold's calculation process used for detecting the hotspot is not described

Table 1 summarizes that the proposed method shows the least installed sensors, while other techniques require more. Fewer sensor installation makes the proposed algorithm becomes simple to implement with less cost. Also, in terms of the detection capability in cell scale, other techniques have limitations. Several points include certain irradiation and configuration limitation.

VI. CONCLUSION

This paper presents the improved hotspot model, which is derived from the elaborate analysis of the reversed bias effect stated in the IEC 61215 standard. The analysis shows the effects of hotspots from the factors, including the shunt resistance, level of irradiation and total performance in the cluster's structure PV module. Results show more development and compatibility of the hotspot's model, contributing to a more practical level with the PV's standard. The implementation and graphical results prove the efficiency and accuracy of the detection in different irradiation and shunt resistances. The algorithm shows fast detection within 5 seconds, representing the inclined average slope. The main challenges are the determination of power dissipation, which requires more elaborate sensors installation and the material property parameters. Future works include the PV material characteristic analysis under hotspot conditions such as thermal distributions and heat transfer on each PV material structure.

REFERENCES

[1] A. M. Salazar and E. Q. B. Macabebe, "Hotspots dtection in photovoltaic modules using infrared termography," in *The 3rd Int. Conf. Manufacturing and Industrial Technologies (ICMIT 2016)*, Istanbul, Turkey, May 2016, pp. 1–5, doi: 10.1051/matecconf/20167010015.

[2] M. Dhimish, P. Mather, and V. Holmes, "Evaluating power loss and performance ratio of hot-spotted photovoltaic modules," *IEEE Trans. Electron Devices*, vol. 65, no. 12, pp. 5419–5427, 2018, doi: 10.1109/TED.2018. 2877806.

[3] D. S. Pillai and N. Rajasekar, "A comprehensive review on protection challenges and fault diagnosis in PV systems," *Renewable & Sustainable Energy Reviews*, vol. 91, pp. 18–40, Aug. 2018, doi: 10.1016/j.rser.2018.03.082.

[4] B. Hossam and K. Itako, "Real time hotspot detection using scan-method adopted with P&O MPPT for PV generation system," in *2016 IEEE 2nd Annual Southern Power Electronics Conf. (SPEC)*, Auckland, New Zealand, Dec. 2016, pp. 1–5, doi: 10.1109/SPEC.2016.7846122.

[5] K. Yedidi, S. Tatapudi, J. Mallineni, B. Knisely, J. Kutiche, and G. TamizhMani, "Failure and degradation modes and rates of PV modules in a hot-dry climate: Results after 16 years of field exposure," in *2014 IEEE 40th Photovoltaic Specialist Conf. (PVSC)*, Denver, CO, USA, Jun. 2014, pp. 3245–3247, doi: 10.1109/PVSC.2014.6925626.

[6] I. U. Khalil, A. U. Haq, Y. Mahmoud, M. Jalal, M. Aamir, M. U. Ahsan, and K. Mehmood, "Comparative analysis of photovoltaic faults and prformance evaluation of its detection techniques," *IEEE Access*, vol. 8, pp. 26676–26700, 2020, doi: 10.1109/ACCESS.2020.2970531.

[7] P. Bharadwaj, K. Karnataki, and V. John, "Formation of hotspots on healthy PV modules and their effect on output performance," in *2018 IEEE 7th World Conf. Photovoltaic Energy Conversion (WCPEC)*, Waikoloa, HI, USA, Jun. 2018, pp. 0676–0680, doi: 10.1109/PVSC.2018.8548126.

[8] S. Deng, Z. Zhang, C. Ju, J. Dong, Z. Xia, X. Yan, T. Xua, and G. Xing, "Research on hot spot risk for high-efficiency solar module," *Energy Procedia*, vol. 130, pp. 77–86, Sep. 2017, doi: 0.1016/j.egypro.2017.09.399.

[9] U. Hoyer, A. Burkert, R. Auer, C. B. Lutz, C. Vodermayer, M. Mayer, and G. Wotruba, "Analysis of PV modules by electroluminescence and IR thermography," in *24th European Photovoltaic Solar Energy Conf. (24th PVSEC)*, Hamburg, Germany, Sep. 2009, pp. 21–25.

[10] L. Antonio and H. Steven, *Handbook of photovoltaic science and engineering,* Chichester, UK: John Wiley & Sons, 2003.

[11] M. Simon and E. L. Meyer, "Detection and analysis of hot-spot formation in solar cells," *Solar Energy Materials & Solar Cells*, vol. 94, no. 2, pp. 106–113, Feb. 2010, doi: 10.1016/j.solmat.2009.09.016.

[12] Y. Wang, K. Itako, T. Kudoh, K. Koh, and Q. Ge, "Voltage-based hot-spot detection method for photovoltaic string using a projector," *Energies*, vol. 10, no. 2, pp. 1–14, 2017, doi: 10.3390/en10020230.

[13] K. A. Kim and P. T. Krein, "Reexamination of photovoltaic hot spotting to show inadequacy of the bypass diode," *IEEE Journal of Photovoltaics,* vol. 5, no. 5, pp. 1435–1441, Sep. 2015, doi: 10.1109/jphotov.2015.2444091.

[14] T. Ghanbari, "Hot spot detection and prevention using a simple method in photovoltaic panels," *IET Generation, Transmission & Distribution*, vol. 11, no. 4, pp. 883–890, Mar. 2017, doi: 10.1049/iet-gtd.2016.0794.

[15] *Terrestrial photovoltaic (PV) modules- design qualification and type approval - Part 1: Test requirements*, IEC 61215-1, 2016.

[16] D. Rossi, M. Omana, D. Giaffreda, and C. Metra, "Modeling and detection of hotspot in shaded photovoltaic cells," *IEEE Trans. Very Large Scale Integration*, vol. 23, no. 6, pp. 1031–1039, Jun. 2015, doi: 10.1109/tvlsi.2014.2333064.

[17] J. Gosumbonggot and G. Fujita, "Partial shading detection and global maximum power point tracking algorithm for photovoltaic with the variation of irradiation and temperature," *Energies*, vol. 12, no. 2, pp. 1–22, Jan. 2019, doi: 10.3390/en12020202.

[18] T. Ghanbari, "Permanent partial shading detection for protection of photovoltaic panels against hot spotting," *IET Renewable Power Generation*, vol. 11, no. 1, pp. 123–131, Sep. 2016, doi: 10.1049/iet-rpg.2016.0294.